Supporting Information

Iron Complexes of a Macrocyclic N-Heterocyclic Carbene/Pyridine Hybrid Ligand

Iris Klawitter,[†] Markus R. Anneser,[‡] Steffen Meyer,[†] Sebastian Dechert,[†] Serhiy Demeshko,[†] Stefan Haslinger, [‡] Alexander Pöthig,[‡] Fritz E. Kühn,[‡,*] Franc Meyer[†,*]

[†] Institute of Inorganic Chemistry, Georg-August-University Göttingen, Tammannstraße 4, D-37077 Göttingen, Göttingen

[‡] Chair of Inorganic Chemistry/Molecular Catalysis, Catalysis Research Center, Technische Universität München, Ernst-Otto-Fischer-Straße 1, D-85747 Garching bei München, Germany

Contents

1. Alternative synthesis of **1**

[1,5(2,6)-dipyridina-3,7(1,3)-imidazoliuma-cycloocatphane] hexafluorophosphate (0.70 g, 1.1 mmol) was dissolved in acetonitrile (10 mL) and the solution cooled to -40 °C. The solution was then transferred via cannula to a flask charged with a suspension of [Fe{N(SiMe$_3$)$_2$}$_2$(THF)] (0.60 g, 1.34 mmol) in acetonitrile (10 mL) at -40 °C. Under stirring, the solution was allowed to warm up to room temperature, and after 6 days at 35 °C a clear, dark solution was obtained. The volume was reduced to by half and an equal amount of diethyl ether was added. The solid precipitate was separated by filtration, and was extracted two times with 10 mL MeCN/Et$_2$O (v:v 1:1). The combined filtrates were concentrated and purified by column chromatography over silica (15 g/MeCN: HPLC-Grade under argon). The first orange band eluted was collected, concentrated and precipitated with an excess of diethyl ether. After washing two times with diethyl ether and drying in vacuum, a yellow powder was obtained (600 mg, 71 % yield).

2. Reaction of **1** with 2-(*tert*-butylsulfonyl)-iodosobenzene

2-(*tert*-Butylsulfonyl)-iodosobenzene (88 mg, 0.26 mmol, 4.0 eq.) was added to a solution of **1** (50 mg, 65 mmol, 1.0 eq.) in MeCN (3 mL) at −40 °C. The solution immediately turned red. A ^{57}Fe Moessbauer spectrum of the frozen reaction mixture at 80 K showed two quadrupole doublets (δ_1 = 0.50 mm s^{-1}, ΔE_{Q1} = 0.90 mms^{-1}, ~70% and δ_2 = 0.21 mm s^{-1}, ΔE_{Q2} = 2.85 mms^{-1}, ~30%) indicative of hs-Fe^{III} or ls-Fe^{II} species (the major component with δ_1 = 0.50 mm s^{-1} likely has no Fe-C^{NHC} bond, because of the high isomer shift), but there was no Mössbauer evidence of an oxoiron(IV) complex such as [L^{1}Fe=O](OTf)$_2$. Also ESI mass spectrometry of the reaction did not show any signal expected for an oxoiron(IV) complex.

3. NMR Spectra

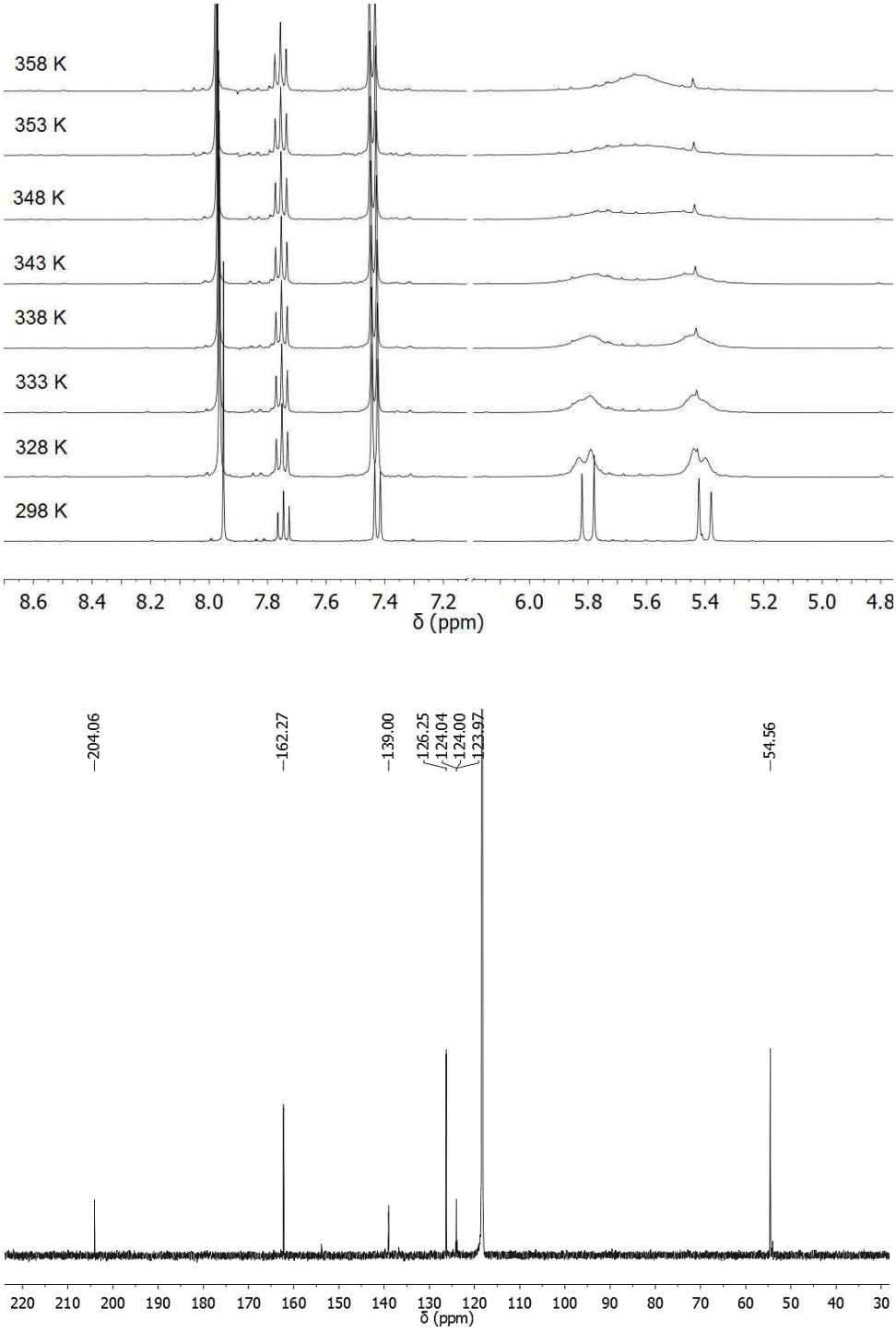

Figure S 1: ^{1}H (top, at different temperatures) and ^{13}C NMR spectra (bottom) of **1** in acetonitrile-d_3.

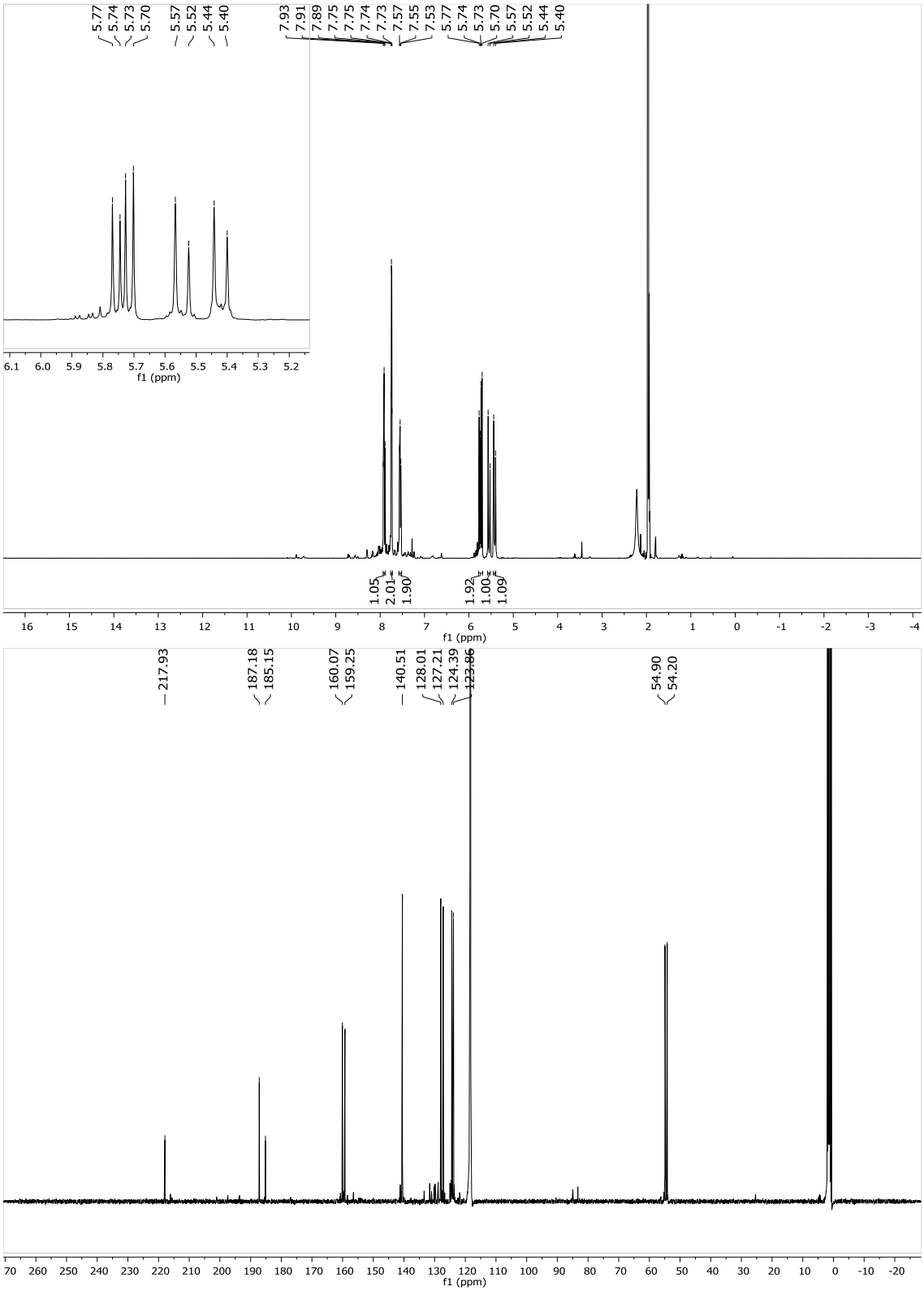

Figure S 2: ^{1}H (top, at different temperatures) and ^{13}C NMR spectra (bottom) of **2** in acetonitrile-d_3.

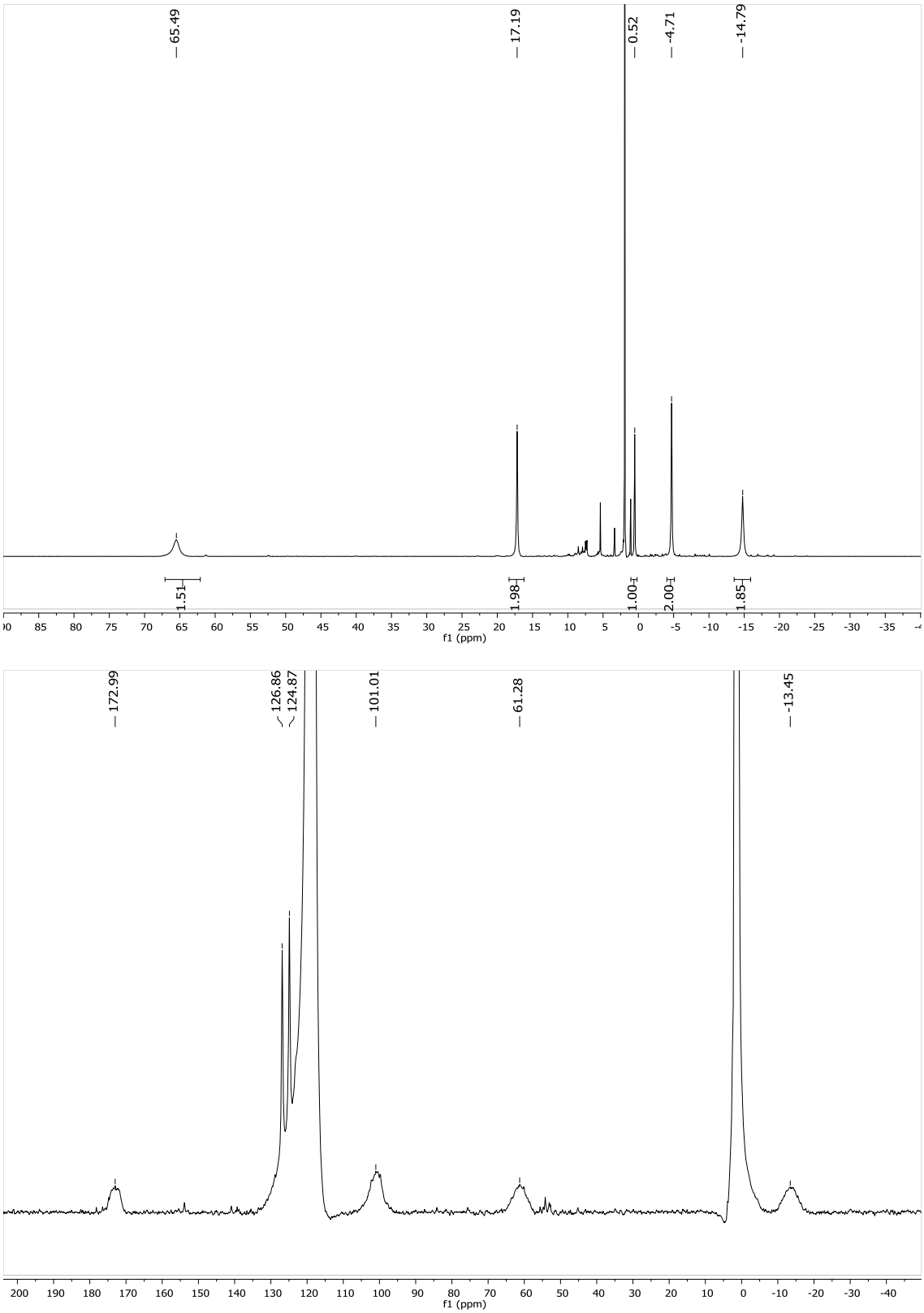

Figure S 3: ^{1}H (top) and ^{13}C NMR spectra (bottom) of **4** in acetonitrile-d_3.

4. Determination of rate constants and thermodynamic parameters for the ring flip of **1**

For slow processes the rate constant *k* can be calculated according to[1]

$$k = \frac{1}{\tau} = \pi \cdot \Delta\nu_{FWHM}$$

with τ as life time, and $\Delta\nu_{FWHM}$ as line width (full width at half maximum). $\Delta\nu_{FWHM}$ was determined by line fitting with *MestReNova* software (Mestrelab Research Inc.).

An approximation for the rate constant k_C at the coalescence temperature T_C with diasterotopic protons separated by $\Delta\nu$ (Hz) and *J*-coupling (Hz) is given by

$$k_C \approx 2.22 \cdot \sqrt{\Delta\nu^2 + 6J^2}.$$

In good approximation Gibb's free energy can be calculated according to

$$\Delta^{\ddagger}G = RT_C \cdot \left(ln\frac{k_b}{h} + ln\frac{T_C}{k_C}\right).$$

An EYRING PLOT (Figure S 4) gives the activation parameters, enthalpy and entropy, of the ring-flip.

$$ln\frac{k}{T} = -\frac{\Delta^{\ddagger}H}{R}\frac{1}{T} + \frac{\Delta^{\ddagger}S}{R} + ln\frac{k_b}{h}$$

Table S 1. Calculated values for *k* at different temperatures *T*.

T (K)	*k* (s^{-1})
298	6.079
328	38.47
333	85.50
338	129.3
343	192.8
48	270.1

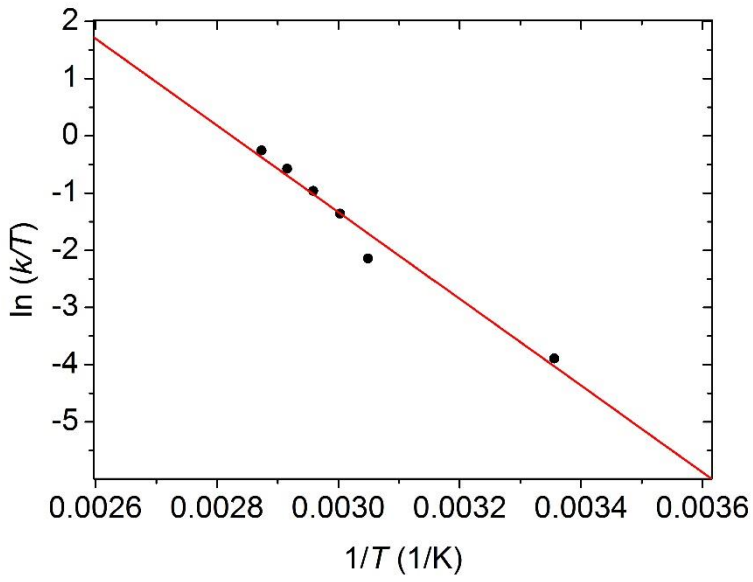

Figure S 4. Eyring plot of the data determined by the variable-temperature NMR measurement. A linear fit for ln(*k*/*T*) versus 1/*T* (slope=-7580.13, intercept=21.4, R^2 = 0.968) resulted in $\Delta S^{\ddagger}$ = -4.7 cal mol^{-1} K^{-1} und $\Delta H^{\ddagger}$ = 15.1 kcal mol^{-1}.

5. Cyclic voltammetry of **1**

Cyclic voltammetry experiments were performed using a BASi $Ag/AgNO_3$ MeCN electrode referenced vs. ferrocene. Under the experimental conditions the Fc/Fc^+ couple, which is a chemically and electrochemically reversible redox couple, shows a peak separation of ΔE^p = 120 mV with a slight dependence on the scan rate. This was considered in data analysis.

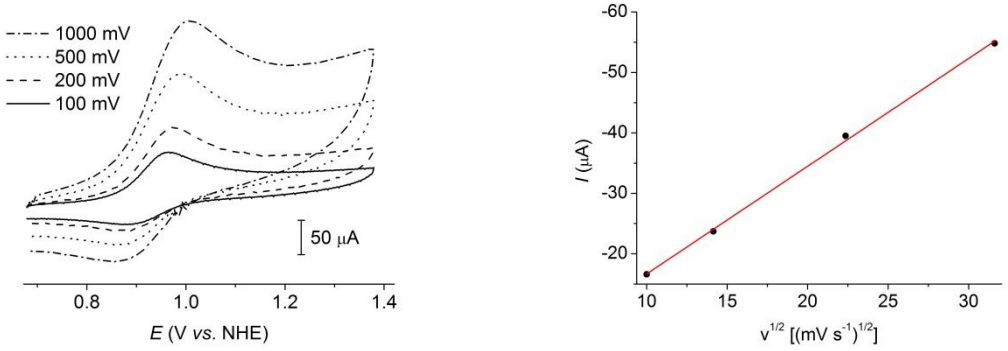

Figure S 5: Left: Oxidation of **1** in acetonitrile (0.1 M nBu$_4$NPF$_6$) at different scan rates. Right: Linear dependence of the current I_{fp} of the forward peak on the square root of the scan rate.

6. IR spectroscopy

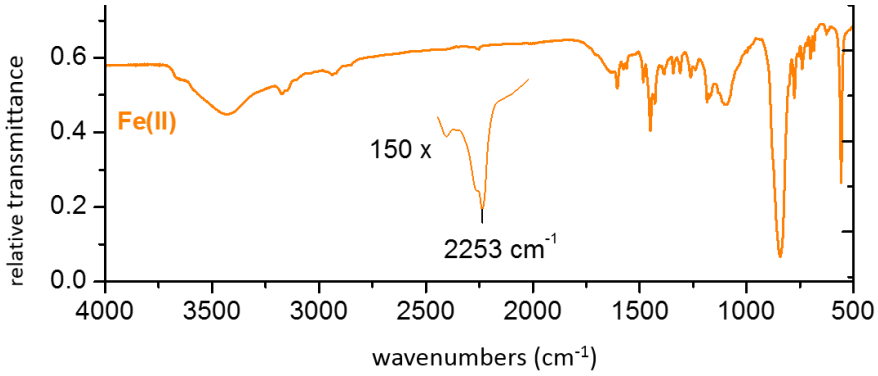

Figure S 6. IR spectrum of $[FeL^1(MeCN)_2](PF_6)_2$ (**1**) recorded as KBr pellet.

7. Mössbauer spectroscopy

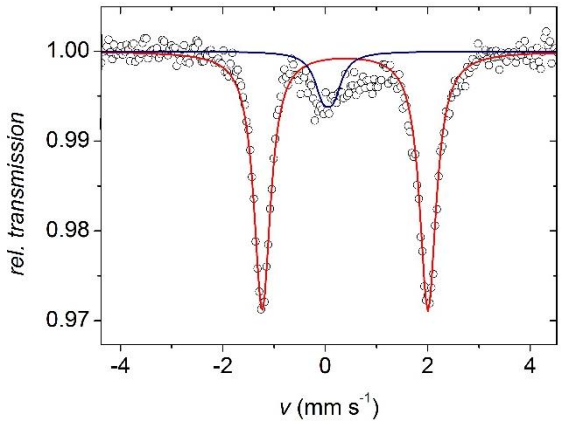

Figure S 7. Zero-field Mössbauer spectrum of solid [FeL^1(N$_3$)$_2$] (**3**) at 80 K (natural abundance ^{57}Fe); the red solid line is a simulation with δ = 0.39 mm s^{-1} and ΔE_Q = 3.24 mm s^{-1} for **3**; the blue line represents 12% of unknown impurity with δ = 0.06 mm s^{-1} and ΔE_Q = 0.21 mm s^{-1}.

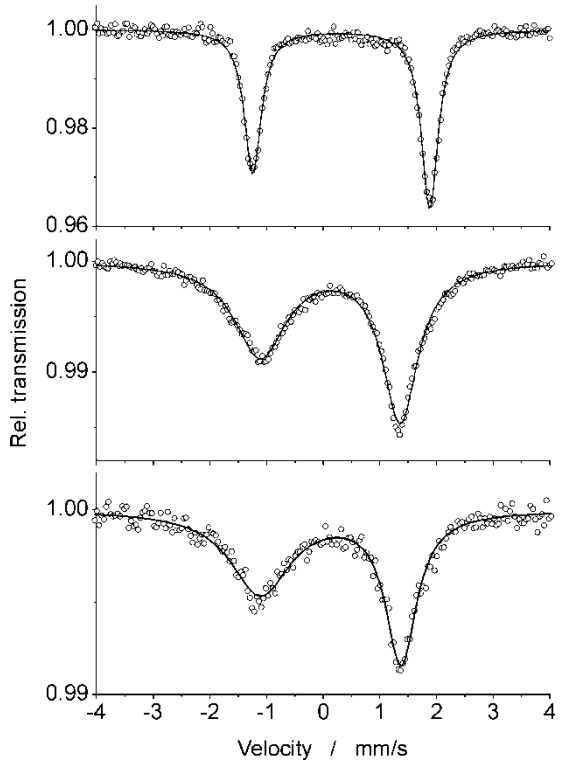

Figure S 8. Zero-field Mössbauer spectrum of [FeL^1(MeCN)$_2$](PF$_6$)$_2$ (**1**; top), of solid [FeL^1(MeCN)$_2$](PF$_6$)$_3$ (**4**; middle), and of a frozen MeCN solution of **1** after oxidation with Th$^{\bullet+}$ClO$_4^-$ (bottom) at 80 K (natural abundance ^{57}Fe); the solid lines represent simulations with δ = 0.32 mm s^{-1}, ΔE_Q = 3.12 mm s^{-1}, line width Γ = 0.36 mm s^{-1} and ratio of intensity left (I_l) to intensity right (I_r) I_l : I_r = 0.81 for **1** (top), δ = 0.13 mm s^{-1}, ΔE_Q = 2.47 mm s^{-1}, line width Γ = 0.76 mm s^{-1}, ratio of intensity left (I_l) to intensity right (I_r) I_l : I_r = 0.87 and ratio of line width left (Γ_l) to line width right (Γ_r) Γ_l : Γ_r = 1.46 for **4** (middle), and δ = 0.13 mm s^{-1}, ΔE_Q = 2.48 mm s^{-1}, line width Γ = 0.66 mm s^{-1}, ratio of intensity left (I_l) to intensity right (I_r) I_l : I_r = 1.09 and ratio of line width left (Γ_l) to line width right (Γ_r) Γ_l : Γ_r = 1.96 for **1** after oxidation with Th$^{\bullet+}$ClO$_4^-$ (bottom).

8. Magnetic measurements

Temperature-dependent magnetic susceptibility measurements for **4** were carried out with a *Quantum-Design* MPMS-XL-5 SQUID magnetometer equipped with a 5 Tesla magnet in the range from 295 to 2.0 K at a magnetic field of 0.5 T. The powdered sample was contained in a gelatin capsule and fixed in a non-magnetic sample holder. Each raw data file for the measured magnetic moment was corrected for the diamagnetic contribution of the gelatin capsule according to $M^{dia}(\text{capsule}) = \chi_g \cdot m \cdot H$, with an experimentally obtained gram susceptibility of the gelatin capsule. The molar susceptibility data were corrected for the diamagnetic contribution according to $\chi_M^{dia}(\text{sample}) = -0.5 \cdot M \cdot 10^{-6}$ cm^3·mol^{-1}.[2] Experimental data were modelled with the *julX* program[3] using a fitting procedure to the spin Hamiltonian $\hat{H} = g\mu_B \vec{B} \cdot \vec{S}$.

Temperature-independent paramagnetism (*TIP*) and paramagnetic impurities (*PI*) with $S = 5/2$ were included according to $\chi_{calc} = (1 - PI) \cdot \chi + PI \cdot \chi_{mono} + TIP$. Best fit parameters are $g = 2.53$, $TIP = 4.2 \cdot 10^{-4}$ cm^{3}mol^{-1} and $PI = 0$ % or, alternatively, $g = 2.27$, $TIP = 4.6 \cdot 10^{-4}$ cm^{3}mol^{-1} and $PI = 3$ %.

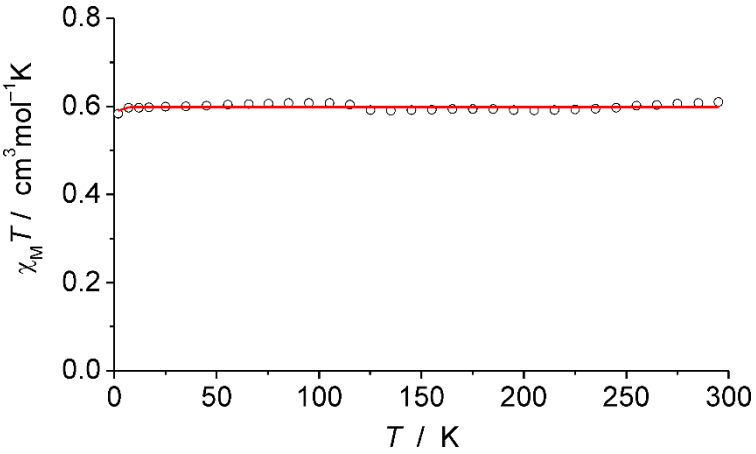

Figure S 9. Temperature dependence of $\chi_M T$ for complex **4**. The solid line shows the simulated data and the empty circles the experimental data.

9. DFT Calculations for complex **1**

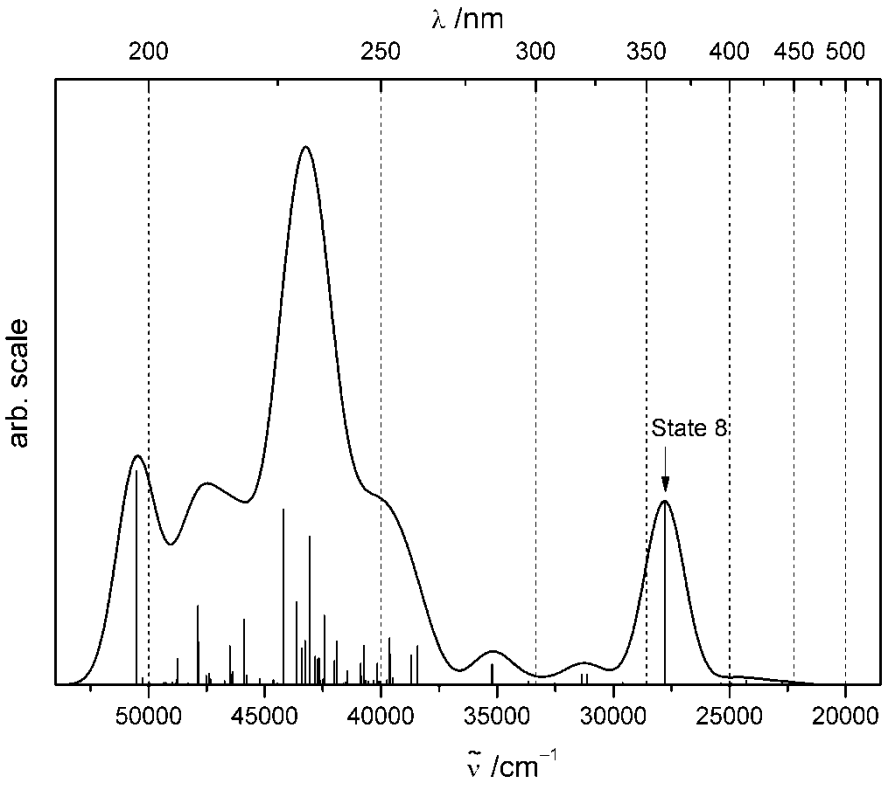

Figure S 10. Calculated absorption spectra of the cation of **1**. The spectra was convoluted using a Gaussian line shape function with a half-width of 2000 cm^{-1}.

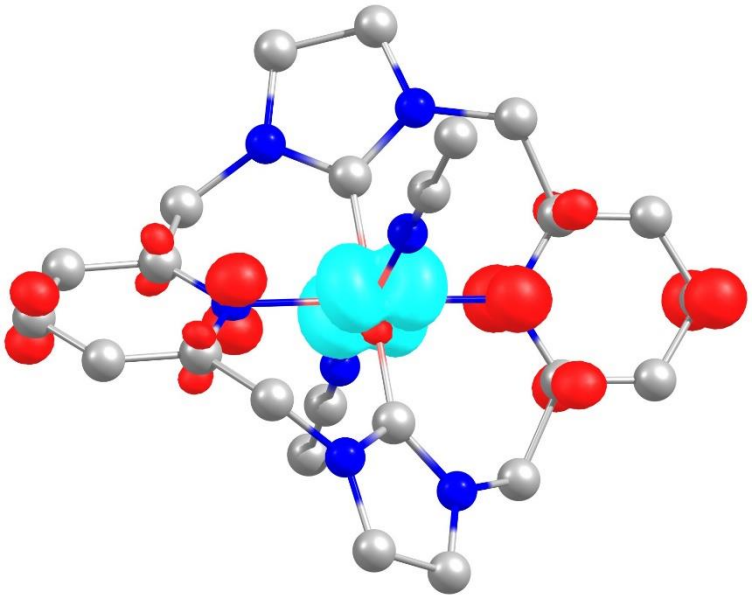

Figure S 11. Calculated TD-DFT difference densities (red/turquoise indicate gain/loss of electron density) of state 8 (27793.3 cm^{-1}, 359.8 nm) (contour value = 0.006, color code: C = grey, N = blue, the central Fe atom is covered by the difference densities).

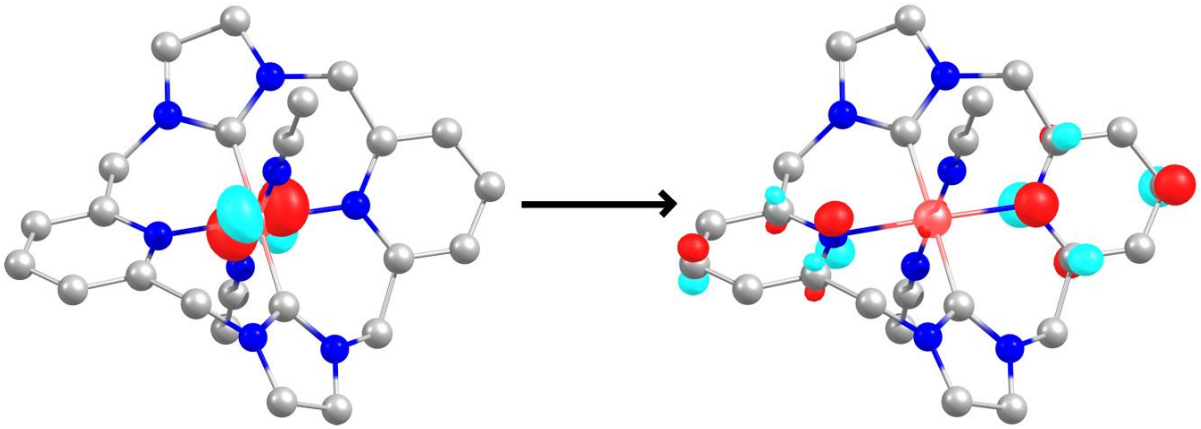

Figure S 12. Natural transition orbitals (occupied/unoccupied pair) that mainly contribute to state 8 (n = 0.83973, 27793.3 cm^{-1}, 359.8 nm) (contour value = 0.09, color code: C = grey, N = blue, Fe = red).

10. DFT Calculations for complex **3**

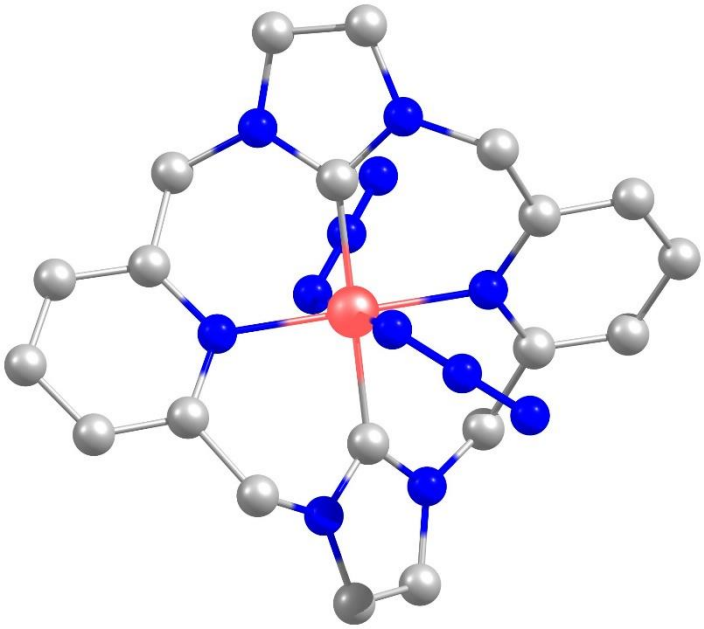

Figure S 13. DFT optimized molecular structure of [LFe(N_3)$_2$] (**3**; color code C = grey, N = blue, Fe = red). Hydrogen atoms not shown.

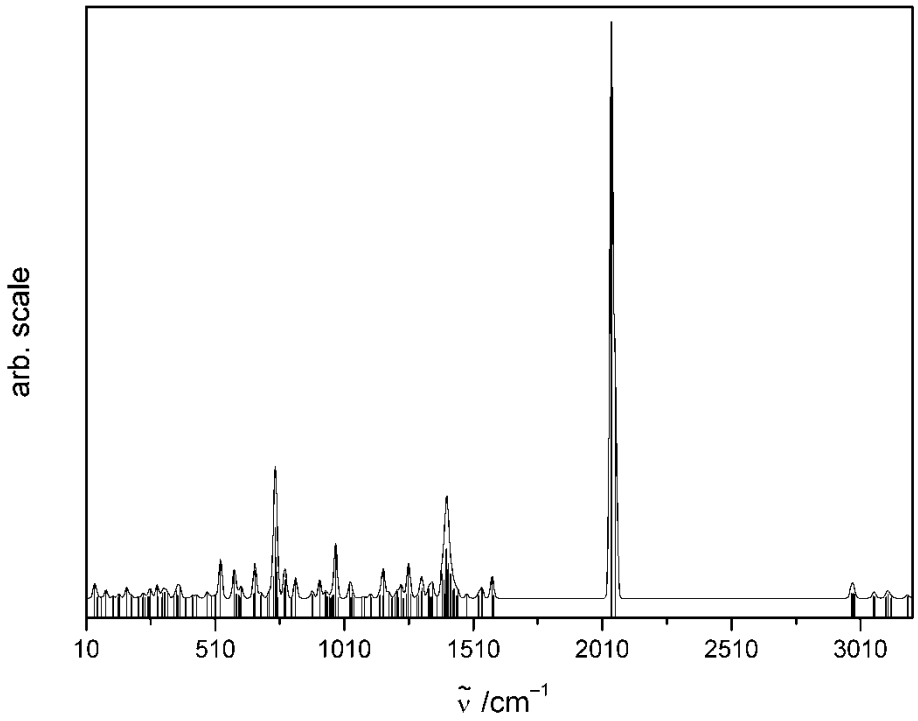

Figure S 14. Calculated IR spectrum of [LFe(N_3)$_2$] (**3**). The spectrum was convoluted using a Gaussian line shape function with a half-width of 15 cm^{-1}.

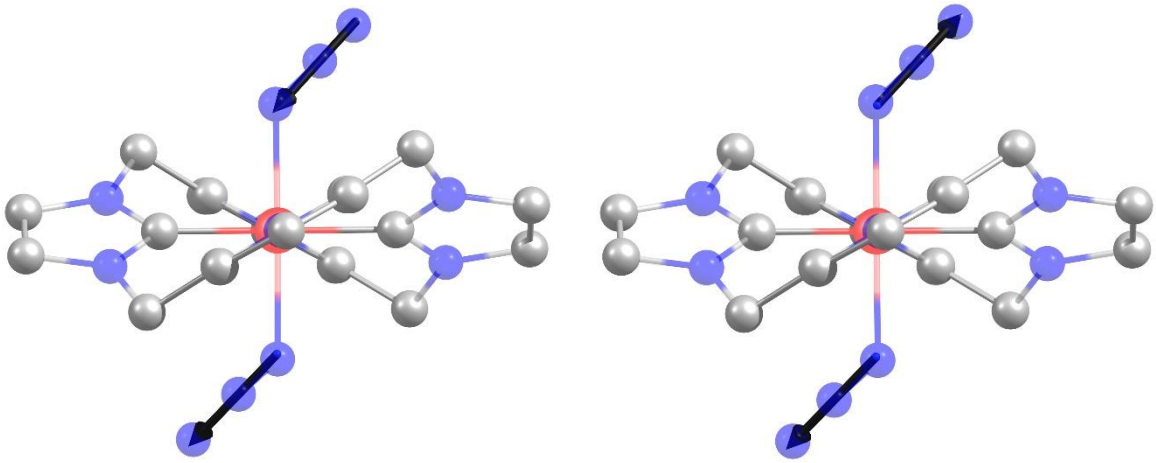

Figure S 15. Displacement vectors (black, visualization threshold = 0.39) of the two prominent IR bands at 2044 cm^{-1} (left) and 2060 cm^{-1} (right) of [LFe(N_3)$_2$] (**3**; color code C = grey, N = blue, Fe = red). Hydrogen atoms not shown.

11. DFT Calculations for complex **4**

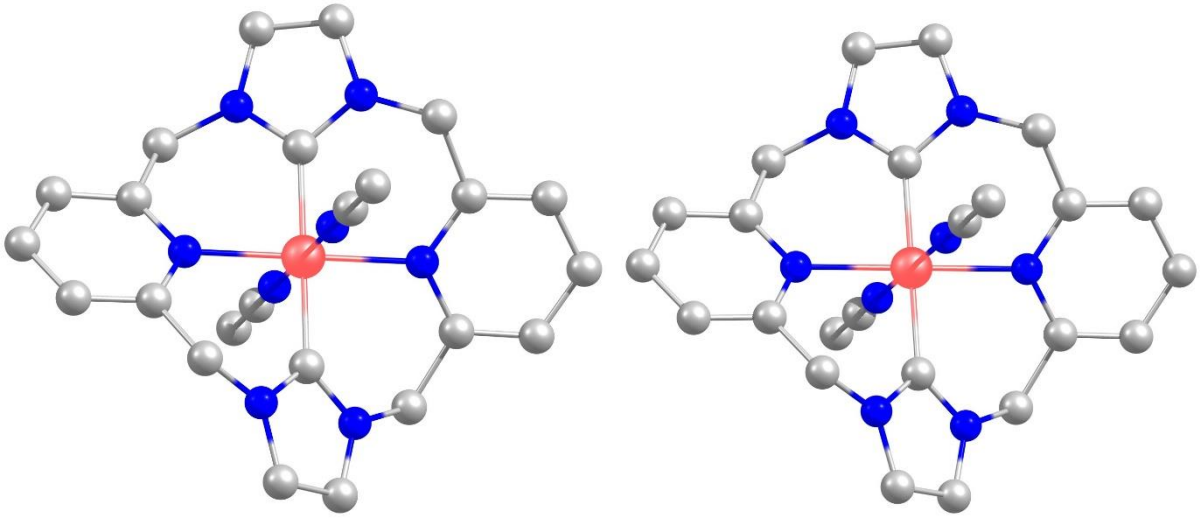

Figure S 16. DFT optimized molecular structures of $[LFe(MeCN)_2]^{3+}$ (cation of **4**) in the S = 1/2 (left) and S = 3/2 (right) states (color code C = grey, N = blue, Fe = red). Hydrogen atoms not shown.

Table S 2: Relative energies of $[LFe(MeCN)_2]^{3+}$ (cation of **4**) in different spin states, obtained by single point calculations.

compound	E_{rel} /kcal mol^{-1}
$[LFe(MeCN)_2]^{3+}$ (S = 1/2)	0
$[LFe(MeCN)_2]^{3+}$ (S = 3/2)	+2

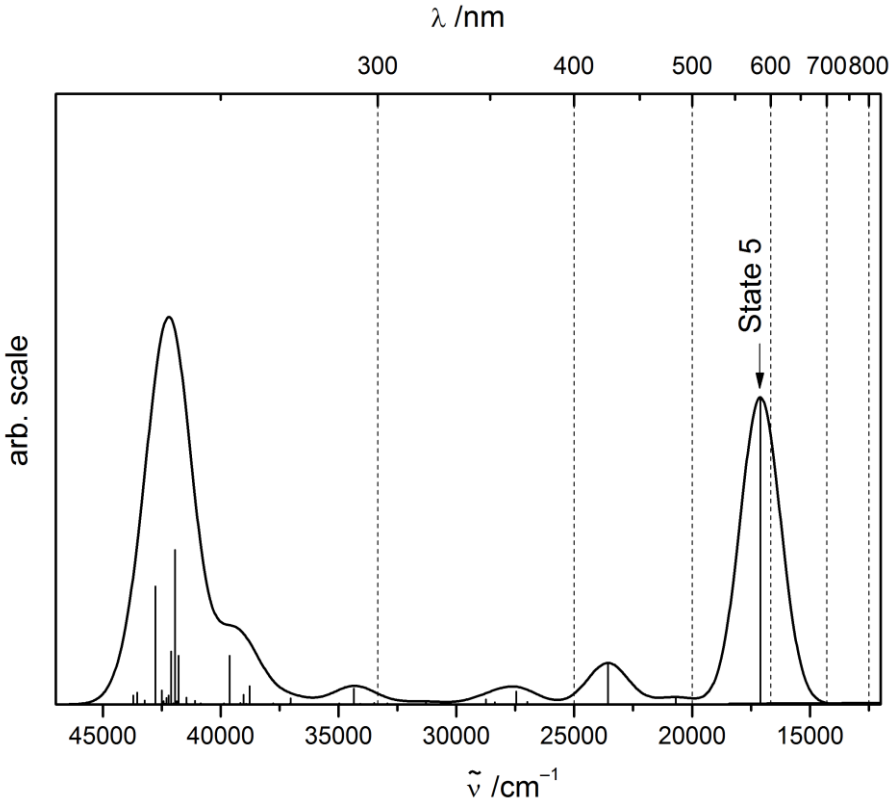

Figure S 17. Calculated absorption spectrum of $[LFe(MeCN)_2]^{3+}$ (cation of **4**; S = 1/2). The spectrum was convoluted using a Gaussian line shape function with a half-width of 2000 cm^{-1}.

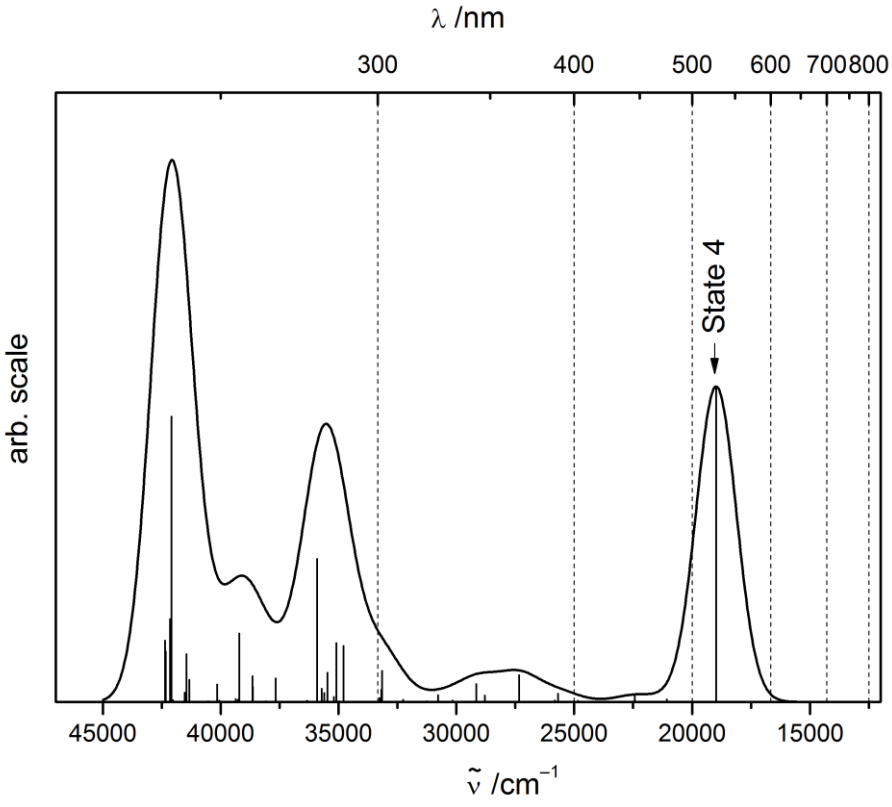

Figure S 18. Calculated absorption spectrum of $[LFe(MeCN)_2]^{3+}$ (cation of **4**; S = 3/2). The spectrum was convoluted using a Gaussian line shape function with a half-width of 2000 cm^{-1}.

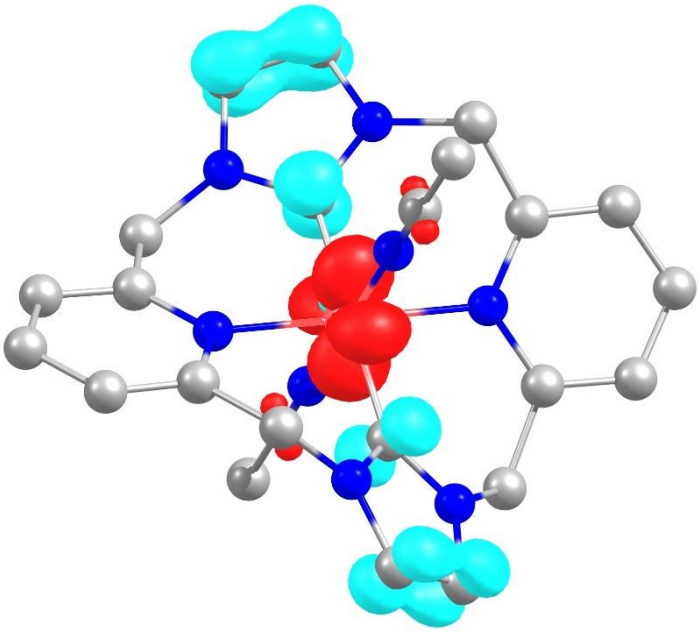

Figure S 19. Calculated TD-DFT difference densities (red/turquoise indicate gain/loss of electron density) of state 5 (17099.7 cm^{-1}, 584.8 nm) in $[LFe(MeCN)_2]^{3+}$ (cation of **4**; *S* = 1/2). (contour value = 0.006, color code: C = grey, N = blue, the central Fe atom is covered by the difference densities).

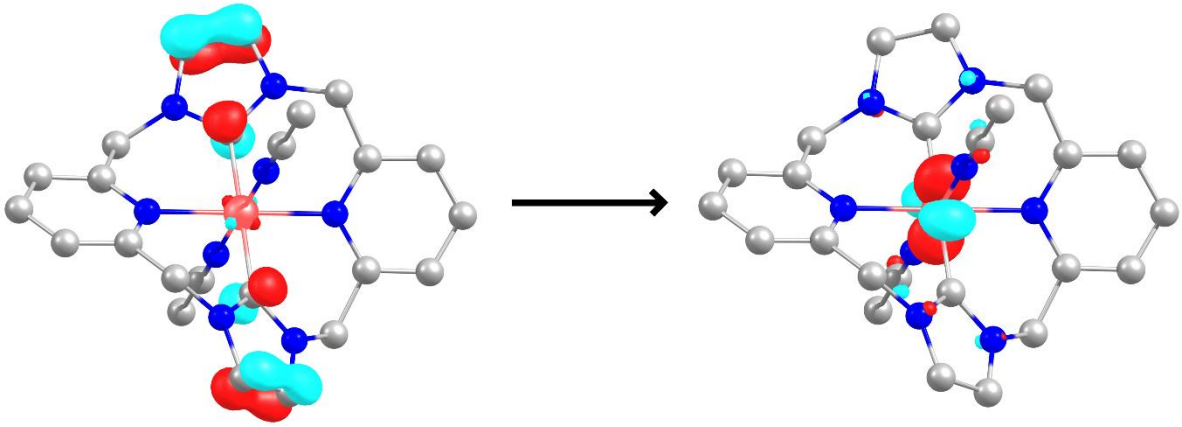

Figure S 20. Natural transition orbitals (occupied/unoccupied pair) that mainly contribute to state 5 (n = 0.9764, 17099.7 cm^{-1}, 584.8 nm) in $[LFe(MeCN)_2]^{3+}$ (cation of **4**; *S* = 1/2) (contour value = 0.08, color code: C = grey, N = blue, Fe=red).

Table S 3: Experimental (exp.) and calculated*) Mößbauer parameters.

compound	δ /mm s^{-1}	ΔE_Q /mm s^{-1}
1 (exp.)	0.32	3.12
$[LFe(MeCN)_2]^{2+}$	0.30	2.99
4 (exp.)	0.13	2.48
$[LFe(MeCN)_2]^{3+}$ (S=1/2)	0.08	2.96
$[LFe(MeCN)_2]^{3+}$ (S=3/2)	0.29	4.24
3 (exp.)	0.39	3.24
$[LFe(N)_3]$	0.30	3.20

*) $\delta = \alpha(\rho - C) + \beta$, with $\alpha = -0.366$, $\beta = 2.852$, $C = 11\,810$, ρ from DFT calculations (see ref. 55)

12. Crystallographic data

General: X-ray data for **1** were collected on a STOE IPDS II diffractometer with an area detector (graphite monochromated Mo-Kα radiation, λ = 0.71073 Å) by use of ω scans at 133 K and for **4** on a Bruker D8 Kappa-ApexII diffractometer with an CCD-detector (graphite monochromated Mo-Kα radiation, λ = 0.71073 Å) by use of φ and ω scans at 123 K (Table S4). The structures were solved using direct methods (SHELXS) and refined against F^2 using all reflections with SHELXL-97[4] (compound **1**) or SHELXL-2014[5] (compound **4**). Non-hydrogen atoms were refined anisotropically. Hydrogen atoms were placed in calculated positions and assigned to an isotropic displacement parameter of 1.2/1.5 U_{eq}(C). Special details: For compound **1**, PF_6^- counter ions were found to be disordered about two positions with occupancy factors of 0.521(2) / 0.479(2). SADI ($d_{P–F}$ and $d_{F\cdots F}$), ISOR and BUMP restraints and EADP constraints were used to model the disorder of the anion. Face-indexed absorption corrections were performed by the program X-RED.[6] For compound **4**, two PF_6^- counter ions were found to be disordered each about two positions with occupancy factors of 0.537(7) / 0.463(7) and 0.855(3) / 0.145(3). SIMU, SAME and DELU restraints were used to model the disorder of the anion. Multi-scan absorption corrections were performed by the program SADABS.[7] The unit cell contains 1 disordered molecule acetonitrile which has been treated as a diffuse contribution to the overall scattering without specific atom positions by SQUEEZE/PLATON.[8]

Table S 4: Crystal data and structure refinement for **1** and **4**.

	1	**4**
empirical formula	$C_{26}H_{27}F_{12}FeN_9P_2$	$C_{28}H_{30}F_{18}FeN_{10}P_3$
formula weight	811.36	997.38
crystal size [mm³]	0.41 × 0.22 × 0.06	0.672 × 0.389 × 0.117
crystal system	triclinic	triclinic
space group	*P*–1	*P*–1
a [Å]	10.6199(7)	11.7825(6)
b [Å]	10.9083(7)	11.8219(5)
c [Å]	15.8956(10)	16.9918(8)
α [°]	101.146(5)	94.757(2)
β [°]	98.988(5)	103.571(2)
γ [°]	115.111(4)	118.684(2)
V [Å³]	1576.01(18)	1964.60(17)
Z	2	2
ρ [g/cm³]	1.710	1.686
F(000)	820	1002
μ [mm^{-1}]	0.688	0.630
T_{min} / T_{max}	0.8251 / 0.9573	0.4912 / 0.7452
θ-range [°]	2.15 - 26.82	2.02 - 25.40
hkl-range	±13, ±13, –20 - 19	±14, ±14, ±20
measured refl.	20187	54372
unique refl. [R_{int}]	6671 [0.0709]	7217 [0.1044]
observed refl. ($I > 2\sigma(I)$)	4901	4737
data / restraints / param.	6671 / 218 / 476	7217 / 171 / 646
goodness-of-fit (F^2)	1.035	1.014
*R*1, *wR*2 ($I > 2\sigma(I)$)	0.0609, 0.1409	0.0592 / 0.1117
*R*1, *wR*2 (all data)	0.0891, 0.1534	0.1084 / 0.1310
resid. el. dens. [e/Å³]	–0.625 / 0.987	-0.653 / 0.602

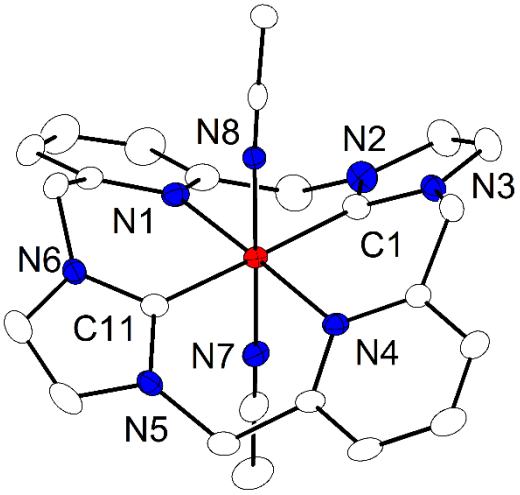

Figure S21. Molecular structure of the cation of **4** (30% probability thermal ellipsoids). Anions and hydrogen atoms have been omitted for clarity.

13. References

[1] a) Sandström, J**.** *Dynamic NMR Spectroscopy;* Academic Press, London, **1982**; b) P. J. Garratt, S. N. Thorn, R. Wrigglesworth, *Tetrahedron* **1994,** *50* (42), 12211-12218.

[2] O. Kahn, *Molecular Magnetism*, VCH Publishers Inc., New York, **1993**.

[3] E. Bill, *julX, Program for Simulation of Molecular Magnetic Data*, Max-Planck Institute for Chemical Energy Conversion,, Mülheim/Ruhr, **2008**

[4] Sheldrick, G.M. *Acta Cryst.* **2008**, *A64*, 112-122.

[5] Sheldrick, G. M. (**2014**). SHELXL2014. University of Göttingen, Germany.

[6] X-RED; STOE & CIE GmbH, Darmstadt, Germany, 2002.

[7] SADABS Version 2014/2. Bruker AXS Inc., Madison, Wisconsin, USA (2014).

[8] Spek, A. L. "PLATON", A Multipurpose Crystallographic Tool, Utrecht University, Utrecht, The Netherlands, (**2010**).